Control of the Reversible Shear-Induced Gelation of Amphiphilic Polymers through Their Chemical Structure

Arnaud Cadix, Christophe Chassenieux,* Françoise Lafuma, and François Lequeux

Physico-chimie des Polymères et des Milieux Dispersés, UMR CNRS 7615, ESPCI 10 rue Vauquelin, 75231 Paris Cedex 05, France

Received August 30, 2004; Revised Manuscript Received October 25, 2004

ABSTRACT: This paper reports on the synthesis and characterization of a series of amphiphilic polymers which exhibit spectacular reversible shear-induced gelation in water. The systems consist of hydrophobically modified copolymers based on *N*,*N*-dimethylacrylamide and acrylic acid. The influence of molecular parameters such as the molecular weight and composition of the terpolymers on the rheological properties has been established. In the linear regime, the polymers behave like classical associating polymers: the sharp increase of the viscosity with concentration is the result of the transformation of intra- into intermolecular associations. Moreover, the dynamics of the physical gels obtained at high concentrations is tremendously slowed by the presence of alkyl side chains. Under shear the solutions display a Newtonian plateau at low shear rate followed by a shear-induced gelation. The latter is characterized in terms of a critical shear rate which sharply decreases as the polymer volume fraction increases. Thus, it appears that the shear-induced gelation may be controlled by adjusting the polymer molecular features. The networks built under shear closely behave like highly concentrated solutions at rest, suggesting a possible parallel between increasing shear and increasing concentration. This latter fact is reminiscent of the situation encountered with wormlike micelles. Shear flow could induce a transition between individual aggregates and a transient network as an increase in concentration does, thanks to the sharp modification of the electrostatic screening at the overlap concentration.

Introduction

In the field of colloids, shear-thickening (i.e., an increase of viscosity under shear) has been reported in various systems such as concentrated suspensions,[1] polymer/particle mixtures,[2] mesophases of surfactants close to a phase transition,[3−5] or wormlike micelles. The latter case has been extensively documented, and several experimental techniques comprising flow birefringence[6] or small angle neutron scattering under shear[7,8] have been used to explain the molecular mechanism for the shear thickening.

When one considers solutions of polymer, most of them display shear thinning. However, shear-thickening behavior has been encountered in polymers dissolved in bad solvents.[9−14] This property is then due to an increase in the fluctuations of concentration under flow, thanks to a coupling between the stress and structure of the fluid.[15] Thus, aggregation of the macromolecules occurs and is further favored by the absence of excluded volume. Associating polymers also exhibit shear-thickening properties near their overlap concentration.[16] An associating polymer consists of a solvophilic polymeric backbone bearing solvophobic groups known as "stickers" which can be either hydrophobic in the case of water-soluble formulations or ionic when ionomers are considered. In solution, to limit contacts with the solvent, stickers self-aggregate into microdomains. Models for associating polymers may be telechelic systems for which the stickers are exclusively located at both ends of the chains. It is generally recognized that at low concentration these systems self-aggregate into flower-like micelles through intramolecular associations. Then, with increasing concentration, a bridging of the micelles occurs, thanks to intermolecular associations which lead to the formation of a physical network. In the same concentration range shear-thickening properties may be observed.[7,17−20] From a theoretical point of view, a mechanism based on non-Gaussian stretching has been suggested, in particular, by Marucci et al.[21] It is believed that if the capture of the dangling ends by the network occurs before they fully relax the strain, a critical shear thickening should appear. Such a mechanism has been found to fairly agree with rheological results obtained on model water-soluble associative thickeners.[20] Shear thickening has also been encountered with associating polymers having a random distribution of their stickers. In the latter case the behavior shown by ionomers is striking: shear-induced gelation may occur, and the gel state can remain for a long time.[22,23] To predict such a transition, Witten et al.[22] proposed a mean field approximation based on an increasing number of intermolecular associations due to the stretching of the polymer chains under flow. However, in summary, it can be said that even for relatively simple macromolecular architectures, the mechanism for shear thickening is still a matter of discussion.

An example of water-soluble polymer which exhibits spectacular shear-thickening properties combines both amphiphilic properties and a limited solubility in water; it consists of a high molecular weight copolymer based on *N*-isopropylacrylamide (NIPAM) (a thermosensitive monomer which exhibits a lower critical solution temperature (LCST) equal to 32 °C when polymerized) and an amphiphilic cationic comonomer.[24] When the temperature is higher than 35 °C, the pNIPAM backbone is in bad solvent conditions and the copolymers display a spectacular shear-induced gelation. A phase separation does not appear since the amphiphilic comonomer

* To whom correspondence should be addressed. E-mail: christophe.chassenieux@espci.fr.

10.1021/ma0482258 CCC: $30.25
Published on Web 12/24/2004

Table 1. Molecular Characteristics of the Precursors *x*DMA/(100 − *x*)AA

sample	$[Na_2S_2O_5]$ mM	M_w (kg/mol)[a]	M_w (kg/mol)[b]	I_p[b]	AA content (mol %)		
					elemental analysis	^{13}C NMR	potentiometry
80DMA/20AA (28)	11.8	28	27	1.6	16	18	16
80DMA/20AA (130)	3.5	130	100	2.1	17	16	15
80DMA/20AA (370)	1.2	370	310	3.7	17	20	18
80DMA/20AA (940)	0.35	940	870	3.3	18	19	16
80DMA/20AA (2200)	0.035	2200	2300	2.8	18	21	17
80DMA/20AA (3100)	0.040	3100	3300	3.1	20	18	18
90DMA/10AA	0.035	3700	2850	2.9	8	9	6
75DMA/25AA	0.035	2480		2.5	25	22	23
65DMA/35AA	0.035	2740	3400	2.8	33	27	28
60DMA/40AA	0.035	2520		2.5	39	33	38
55DMA/45AA	0.035	2160	/	3.1	47	40	45

[a] Measured by SLS under sodium salt form (NaCl 10 mM). [b] Measured by SEC under acidic form ($LiNO_3$ 0.5 M).

prevents it. Furthermore, the shear-induced gelation can then be delayed in terms of temperature by increasing the content of pNIPAM.

On the basis of the conclusions of the studies carried out on these NIPAM copolymers, our objective was to synthesize a family of amphiphilic copolymers which may display shear-induced gelation. To achieve this goal, high molecular weight amphiphilic polymers exhibiting a limited solubility in water need to be considered. Therefore, we chose a random copolymer of *N*,*N*-dimethylacrylamide (DMA) and acrylic acid (AA), the latter units being partially hydrophobically modified. The synthesis route, which is described in detail below, allows us to easily tune the molecular weight of the polymer backbone and its composition in terms of both the hydrophobic and the charge contents. The influence of each of these parameters on the rheological properties of the solutions at rest and under flow has been systematically studied as described below. Last, we established that shear-induced gelation is reversible. This reversibility is again very sensitive to the molecular features of the polymer as pointed out in the last section of this paper. A parallel between these systems and wormlike micelles may be drawn as pointed out in the Discussion of this paper.

Experimental Section

Chemicals.

N,*N*-Dimethylacrylamide (DMA), *n*-tetradecylamine, *n*-hexadecylamine, and *n*-octadecylamine were purchased from Aldrich, and dicyclohexylcarbodiimide (DCCI) was purchased from Acros. Acrylic acid (AA) and *n*-dodecylamine were provided by Fluka. All solvents have been purchased from SDS and used as received.

Synthesis of Polymers.

Synthesis of the polymers occurs in two steps. In the first one a precursor copolymer based on DMA and AA was synthesized. In the second step a part of the AA units was hydrophobically modified. As an example, the synthesis of a precursor based on 80 mol % of DMA and its hydrophobic modification with 10 mol % of dodecyl side chains with a molecular weight of 130 kg/mol is given below.

(a) Synthesis of the Precursor (80 DMA/20 AA).

Into a 500 mL three-necked round-bottom flask, 26 g (0.264 mol) of DMA and 4.7 g (0.066 mol) of AA were mixed with 220 mL of water. The pH is adjusted between 8 and 10 by adding 20 mL of 1M NaOH. The homogeneous mixture obtained by magnetic stirring was deaerated with argon for 30 min. A 0.72 g (3.2 mmol) amount of ammonium persulfate and 180 mg (0.95 mmol) of sodium metabisulfite were added. The polymerization proceeds for 90 min at 30 °C. A 10 mL amount of 3 M HCl was then added, and the polymer was dialyzed against pure water for 1 week. Finally, the polymer was recovered by freeze drying. The yield of polymer was 70%.

The content of AA incorporated in the precursor is estimated by elemental analysis, ^{13}C NMR spectra, and potentiometric measurements. The weight-average molecular weight (M_w) of the polymer under the acidic form and the polydispersity index (I_p) were determined by size exclusion chromatography (SEC) using a universal calibration procedure and viscosity detection with 0.5 M $LiNO_3$ as the solvent. Furthermore, static light-scattering (SLS) measurements allow the measurements of M_w for the polymer under the sodium salt form. The agreement between both SEC and SLS is fair (see Table 1).

(b) Hydrophobic Modification of the Precursor (80DMA/10AA/10C12).

Into a 500 mL round-bottom two-necked flask, 6 g of precursor was dissolved overnight in 200 mL of *N*-methyl-2-pyrrolidone (NMP) at 70 °C. A 1.2 g (6.5 mmol) amount of *n*-dodecylamine dissolved in 10 mL of NMP and 7.9 g (39 mmol) of DCCI dissolved in 10 mL of NMP were added. The reaction mixture was heated at 70 °C for 12 h. The polymer solution was then poured in 3 L of diethyl ether, filtered, and dried under vacuum. The dried polymer was dissolved in 300 mL of chloroform and poured again in 3 L of diethyl ether. This process was repeated twice. Then the polymer was dissolved in 500 mL of deionized water, and a small excess of 1 M NaOH was added to neutralize the remaining acrylic acid units. The solution was dialyzed against water for 1 week, and the polymer was recovered by freeze drying. The grafting content was determined by ^1H NMR and elemental analysis.

The solutions of the samples were prepared with ultrapure water (Milli-Q- grade). In the case of the precursors equilibrium is reached within a few days, whereas for the hydrophobically modified polymers one needs to wait several weeks prior to measurements. In the latter case, magnetic stirring of the samples is obviously prohibited.

Nomenclature.

In the following a precursor consisting of x mol % of *N*,*N*-dimethylacrylamide will be denoted xDMA/(100 − x)AA. Its hydrophobic modification with y mol % of alkyl side chains comprising n carbons leads to a terpolymer denoted xDMA/(100 − x − y)AA/yCn. The weight-average molecular weight of the precursor measured by SLS appears in parentheses after the notation of the polymer.

For example, 80DMA/10AA/10C12 (3100) corresponds to a terpolymer whose composition is 80 mol % of DMA, 10 mol % of AA, and 10 mol % of dodecyl pendants with a weight-average molecular weight of 3100 kg/mol (see Figure 1).

Basically, this means that our systems combined three kinds of monomers: electrostatic (the AA units are under sodium salt form), hydrophilic, and hydrophobic ones.

Rheological Measurements.

Depending on the viscosity of the samples, two strain-imposed rheometers were used.[25] A Low Shear 30 from Contraves measures the viscosity for low viscous solutions, whereas a Rheometrics Fluid Spectrometer II (RFSII) allows the study of more viscous samples. In both cases, Couette geometries were used with a gap of 0.5 (LS 30) and 0.25 mm

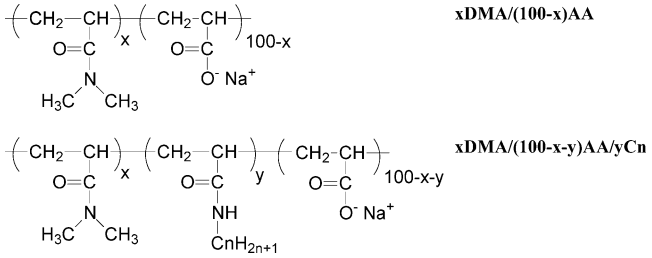

Figure 1. Chemical structures of the hydrophobically modified terpolymers *x*DMA/(100 − *x* − *y*)AA/*y*C*n* and of their precursors *x*DMA/(100 − *x*)AA. *x* ranges from 55 to 90 mol %, *y* ranges from 1 to 15 mol %, and *n* ranges from 12 to 18 carbons.

(RFSII). All samples display a Newtonian behavior at low shear rate (i.e., in the linear regime) which is used to get an estimate of the specific viscosity η_{sp}.

Dynamic measurements were done in the linear viscoelastic regime using a cone and plate geometry (Angle 0.04 rad, diameter 25 or 50 mm) with the RFSII rheometer. All measurements were run at 25 °C unless otherwise specified.

The shear thickening properties were evaluated in terms of a critical shear rate $\dot{\gamma}_c$ (see Figure 7) which corresponds to the shear rate value where the viscosity diverges (an easy way to get an estimate of $\dot{\gamma}_c$ is to find the maximum for the derivative of the viscosity with respect to $\dot{\gamma}$). Prior to flow measurements a dynamic frequency sweep was run to ensure that the samples have reached an equilibrium state. Then, the shear was increased linearly with time using a rate of 10 s^{-1} min^{-1}. Actually, the latter parameter must remain low enough to make the value of $\dot{\gamma}_c$ independent of the history felt by the sample. The relative error for $\dot{\gamma}_c$ is estimated to be 20%. As already pointed out in the literature,[26] measurements of $\dot{\gamma}_c$ are very sensitive to shear history. We are fully aware that results substantially depend on the experimental procedure; that is why it should be emphasized that the values given for $\dot{\gamma}_c$ are more indicative than absolute ones. However, these values can be qualitatively compared as done in the following.

Results

I. Precursor Synthesis.

The molecular characteristics of the precursors are summarized in Table 1. For the fixed composition 80DMA/20AA good control of the molar mass of the polymer has been achieved by adjusting the concentration of reducing agent used as initiator as already shown with several other acrylic monomers.[27]

In all cases the different methods used to estimate the incorporation of AA units fairly agreed but the values are slightly lower than expected. However, all the 80DMA/20AA precursors show roughly the same composition, which makes them suitable for comparisons. In the same way, comparisons for precursors with varying composition can be achieved since the molecular weight is of the same order for all samples.

We do not know the reactivity ratios of the comonomers, and the microstructure of the polymer chains is difficult to establish by ^{13}C NMR due to the complexity of the DMA signals.[28−30] Nevertheless, an analogy with the pair acrylamide/acrylic acid may be drawn. In this case, the reactivity ratios are strongly pH dependent: $r_{acrylamide} = 1.32$ and $r_{acrylic\ acid} = 0.35$ in basic conditions.[31] The consequence on the microstructure of the chains is that the formation of DMA blocks is favored; the copolymers are thus not ideally random ones.

II. Hydrophobic Modification.

Table 2 gives the molecular characteristics of the hydrophobically modified copolymers. The grafting contents which have been determined by ^1H NMR and elemental analysis are close to those expected. Again, for a given series of homologues, comparisons are fair since no big differences in composition are observed.

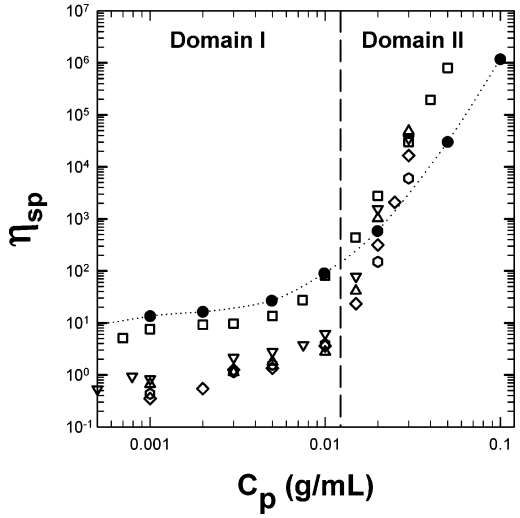

Figure 2. Concentration dependence of the specific viscosity for 80DMA/(20 − *y*)AA/*y*C_{12} (3100) for various alkyl content with $y = 0$ (●), 1 (□), 2 (▽), 5 (△), 10 (◇), and 15 mol % (○). Domain I and domain II correspond to the two concentration regimes that can be discriminated (see text).

III. Rheological Properties in the Linear Regime.

Figure 2 shows the concentration dependence of the specific viscosity (η_{sp}) for the series 80DMA/(20 − *y*)-AA/*y*C12 with the highest molecular weight investigated. Results are compared with the behavior of the precursor. In both cases, two concentration regimes can be discriminated.

Below 7×10^{-3} g/mL the viscosity of the precursor slightly depends on the polymer concentration (C_p), whereas above $C_p = 10 \times 10^{-3}$ g /mL the concentration dependence gets more pronounced. Due to the polyelectrolyte nature and the molecular weight of the chains, the concentration range investigated here is far above the critical overlap concentration (C^*). This means that for the precursor the change in the concentration dependence of the viscosity corresponds to the transition between the nonentangled and the entangled semidilute regimes.

If the hydrophobically modified polymers are now considered, the effect of the hydrophobic modification is weak if the grafting content remains below 1 mol %. Above this value, at low concentration (domain I), η_{sp} slightly increases with concentration and remains 1 order of magnitude lower than the viscosity of the precursor. This shrinkage of the chains is due to very effective intramolecular associations. At higher concentration (domain II) the specific viscosity sharply increases with concentration and even overtakes the viscosity of the precursor. This behavior has been frequently encountered with associating polymers and is claimed to be due to the transformation of intramolecular into intermolecular associations. It can be seen that when the alkyl content ranges from 5 to 15 mol %, the remaining charges have only a slight effect on the overall behavior of the chains.

The influence of the molecular weight of the polymer chains on the specific viscosity has been studied along a wide concentration range for the 80DMA/10AA/10C12

Table 2. Molecular Characteristics of the Hydrophobically Modified Polymers

sample	precursor	alkyl content (mol %)	
		^{1}H NMR	elemental analysis
80DMA/10AA/10C12 (130)	80DMA/20AA (130)	8.6	12.1
80DMA/10AA/10C12 (940)	80DMA/20AA (940)	6.4	11.4
80DMA/10AA/10C12 (2200)	80DMA/20AA (2200)	8.6	11.1
80DMA/10AA/10C12 (3100)	80DMA/20AA (3100)	9.4	10.2
80DMA/19AA/1C12 (3100)	80DMA/20AA (3100)	1.2	1.2
80DMA/18AA/2C12 (3100)	80DMA/20AA (3100)	4.2	2.3
80DMA/15AA/5C12 (3100)	80DMA/20AA (3100)	5.6	5.1
80DMA/5AA/15C12 (3100)	80DMA/20AA (3100)	13.7	14.2
80DMA/15AA/5C14 (3100)	80DMA/20AA (3100)	5.5	5.2
80DMA/15AA/5C16 (3100)	80DMA/20AA (3100)	6.3	5.2
80DMA/15AA/5C18 (3100)	80DMA/20AA (3100)	6.0	5.3
90DMA/10C12	90DMA/10AA	6.0	8.5
75DMA/15AA/10C12	75DMA/25AA	6.1	10
65DMA/25AA/10C12	65DMA/35AA	8.4	9.0
60DMA/30AA/10C12	60DMA/40AA	8.0	13
55DMA/30AA/10C12	55DMA/45AA	6.8	13

series as seen in Figure 3. At low concentration (domain I) the results can be superimposed on the same curve

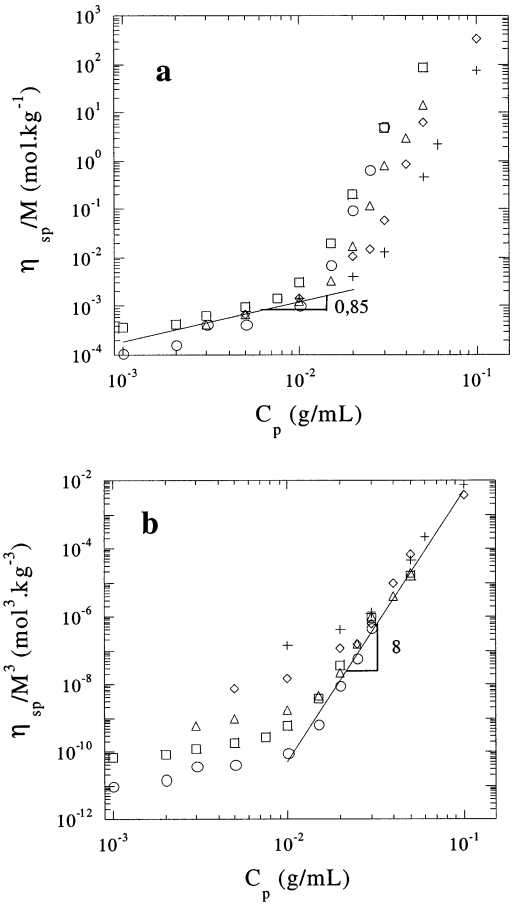

Figure 3. Concentration dependence of the specific viscosity for 80DMA/10AA/10C$_{12}$ with various molecular weights. Data have been rescaled by M (a) or by M^3 (b) to superimpose, respectively, in the low- and high-concentration regime. M = 1.3×10^5 (+), 3.7×10^5 (◇), 9.4×10^5 (△), 2.2×10^6 (□), and 3.1×10^6 g/mol (○).

by rescaling the specific viscosity with the molecular weight (Figure 3a). Thus, in the concentration range where intramolecular associations significantly compact the polymer chains, $\eta_{sp} \approx C_p^{0,85}M^1$. If one rescales the viscosities by M^3, the values obtained in domain II become independent of the molecular weight (Figure 3b) and the variation of the specific viscosity is given then by $\eta_{sp} \approx C_p^8 M^{-3}$.

The sharp increase of the viscosity in domain II is concomitant with the appearance of some viscoelastic properties. At low concentration and low frequency, a Maxwellian behavior is measured. In addition, some fast modes superimpose with the slower mode of relaxation at higher frequencies. The coordinates (ωc, Gc) of the crossing point between G' and G'' give an estimate for the fluid of both the terminal relaxation time ($\tau = 2\pi/\omega c$) and the plateau modulus ($G_0 = 2Gc$).[32] Figure 4 represents the concentration dependence of G_0 and τ for

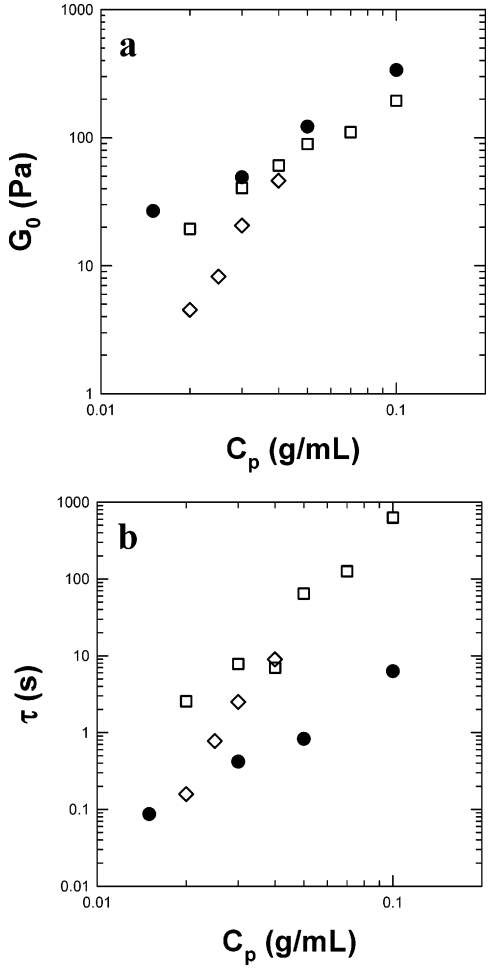

Figure 4. Concentration dependence of the plateau modulus (G_0) (a) and terminal relaxation time τ (b) for 80DMA/(20 − y)AA/xC$_{12}$ (3100) with y = 0 (●), 1 (□), and 10 mol % (◇).

both a weakly (1 mol %) and a highly (10 mol %) hydrophobically modified polymer. Results are compared with the behavior of their precursor.

When one considers the concentration dependence of G_0 (Figure 4a), both the precursor and the weakly hydrophobically modified polymer ($y = 1$) show the same behavior: $G_0 \approx C^{1.4}$. This means that the topology of the network made of entangled chains is poorly affected by a small content of hydrophobic alkyl side chains. Furthermore, in both cases the concentration dependence of the terminal relaxation time is roughly the same (Figure 4b), but one can clearly see that the dynamic is tremendously slowed by the presence of the alkyl side chains. This phenomenon, known as sticky reptation, is due to the presence of intermolecular hydrophobic associations which alter the dynamics without affecting the overall topological properties of the network.

For the highly hydrophobically modified polymer ($y = 10$), the concentration range investigated corresponds to the crossover regime where intramolecular associations turn into intermolecular ones, which deeply affects the concentration dependence of both the terminal relaxation time and the plateau modulus. The predominance of the intramolecular associations at the lowest concentrations investigated accounts for lower values of G_0 when results are compared with the precursor and the weakly hydrophobically modified homologue.

The concentration dependencies of G_0 and τ which have been measured over a wide range of molecular weights are represented in Figure 5. On one hand, G_0 seems to be independent of the molecular weight but increases with the polymer concentration as $C_p^{3.7\pm0.4}$ (Figure 5a). On the other hand, τ is strongly molecular-weight dependent and it is possible to superimpose all the experimental data on a single curve by rescaling τ by M^3. The variation of τ is then given by $M^3C_p^{4.9\pm0.3}$ (Figure 5b).

To conclude this part regarding the influence of the molecular weight and concentration on the linear properties, it should be noted that agreement is obtained between our experimental results and a recent extensive model[33] of the different regimes expected for the concentration dependence of the dynamic properties of associating polymers for both entangled and nonentangled systems. Two main ingredients concomitant with an increase of the concentration have been taken into account. The first one is the transformation of intra- into intermolecular associations with the increase of the concentration, which results in an increasing number of sticky points and a sharp concentration dependence of both the viscosity and the terminal relaxation time. The second fact is a concentration dependence of the lifetime of the hydrophobic associations. Actually the probability for a given sticker to be aggregated increases with concentration; thus, the possibility of finding a new partner for a given sticker decreases and the lifetime of the hydrophobic association significantly increases. Table 3 summarizes the scaling laws predicted in the framework of this model; theoretical predictions are compared with our experimental results. In the high-concentration range (domain II) fair agreement exists between the experimental scaling laws and the behavior expected. In domain I we were not able to measure the variation of both G_0 and τ. However, the concentration dependence for the viscosity disagrees with the scenario for the nonentangled regime of the model[33] and is more similar to the classical behavior of nonentangled polyelectrolytes.[34]

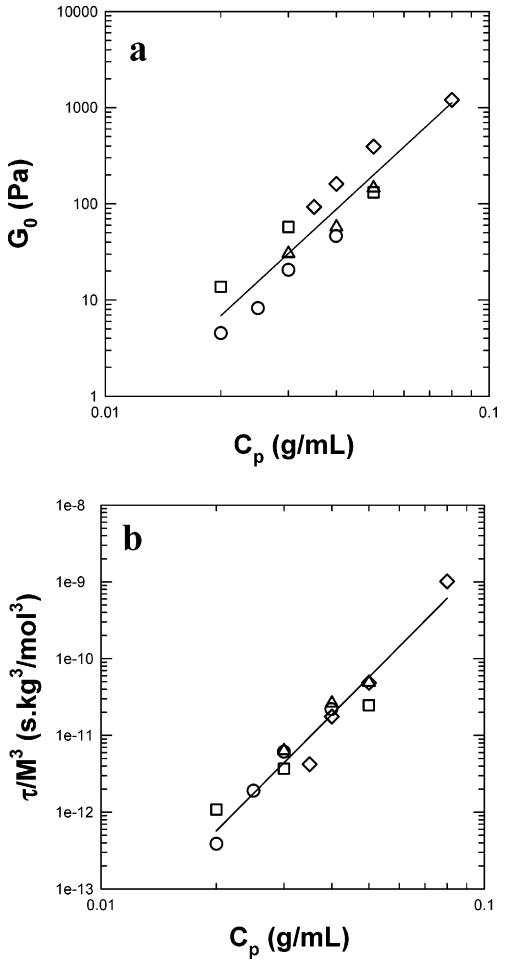

Figure 5. Concentration dependence of the plateau modulus (G_0) (a) and terminal relaxation time τ (b) for various molecular weights of 80DMA/10AA/10C12. In b data have been rescaled by M^3. Symbols are the same as in Figure 3. Straight lines correspond to fits according to $G_0 \approx C_p^{3.7\pm0.4}$ and $\tau \approx M^3C_p^{4.9\pm0.3}$

Influence of the Composition of the Terpolymers.

When the grafting ratio is kept constant to 5 mol % with various alkyl side chains, in the low-concentration range (domain I) the specific viscosity does not systematically depend on the alkyl side chains length (results not shown). In domain II the increase in the associating properties become more pronounced as the length of the alkyl side chains increases, which is a classical result encountered with associating polymers.[35]

Figure 6 shows the concentration dependence of the specific viscosity for polymers with various alkyl contents. When the precursors are considered, the viscosity increases with the charge density, whereas for their hydrophobically modified homologues, at low concentration (domain I) the tendency is the opposite. Nevertheless, the increase in the viscosity with the concentration in domain II gets more pronounced when the charge density increases. This effect will be discussed later.

Finally, at rest the hydrophobically modified polymers show two concentration regimes. At low concentrations (domain I) the behavior is close to what is expected for nonentangled polyelectrolytes collapsed by intramolecular hydrophobic association. For higher concentrations (domain II) the polymers become entangled, which is

Table 3. Scaling Laws Predicted by Rubinstein et al.[33] for the Rheological Properties of Associating Polymers in the Semidilute Entangled and Nonentangled Regimes[a]

	nonentangled regime		entangled regime		experimental results
	intra−inter	inter	intra−inter	inter	$C_p > C_\eta$
η	$MC^{5.9}$	$MC^{1.15}$	$M^3C^{8.5}$	$M^3C^{3.75}$	M^3C^8
τ	$M^2C^{4.9}$	$M^2C^{0.15}$	$M^3C^{6.2}$	$M^3C^{1.45}$	$M^3C^{4.9\pm0.3}$
G_0	$M^{-1}C$	$M^{-1}C$	$C^{2.3}$	$C^{2.3}$	$C^{3.7\pm0.4}$

[a] Predictions are compared with experimental results obtained on the 80DMA/10AA/10C12 series.

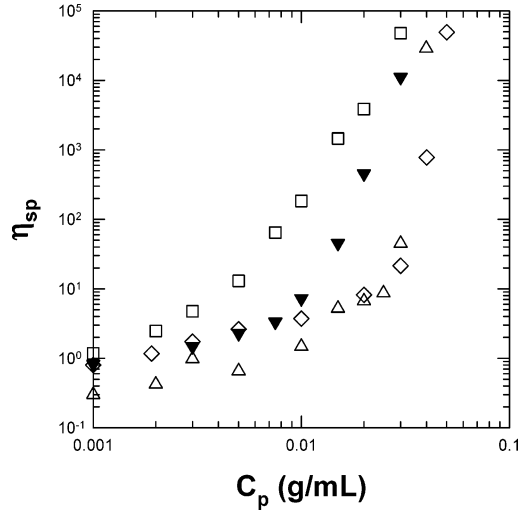

Figure 6. Concentration dependence of the specific viscosity for terpolymers with various charge densities: 90DMA/10C12 (□), 80DMA/10AA/10C12 (▼), 75DMA/15AA/10C12 (△), and 65DMA/25AA/10C12 (◇).

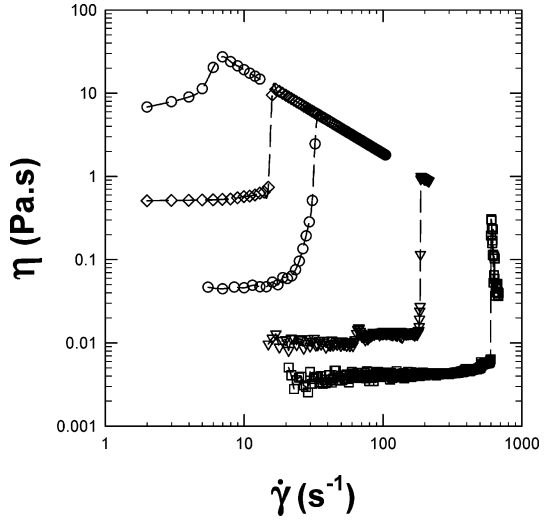

Figure 7. Rheograms obtained for 80DMA/10AA/10C12 (2200) at various concentrations. C_p = 5 (□), 10 (▽), 15 (Δ), 20 (◇), and 30 g/L (○).

concomitant with the transformation of intramolecular associations into intermolecular ones.

IV. Shear-Induced Gelation.

Figure 7 represents typical rheograms obtained for 80DMA/10AA/10C12 (2200) at various concentrations. Let us first consider the lowest concentration investigated. Below roughly 200 s^{-1} the solution behaves like a Newtonian fluid since the viscosity does not depend on the shear rate. The slight increase of the viscosity, which can be observed above 200 s^{-1}, is attributed to nucleation of the gel phase inside the Couette geometry. At 600 s^{-1}, which corresponds to the critical shear rate value ($\dot{\gamma}_c$), the viscosity suddenly gains at least 2 orders of magnitude. Then the solution exhibits a yield−stress behavior ($\eta \approx 1/\dot{\gamma}$), indicating the possibility of wall slipping. That is why it is actually difficult to get an estimate of the amplitude of the increase of viscosity under shear.

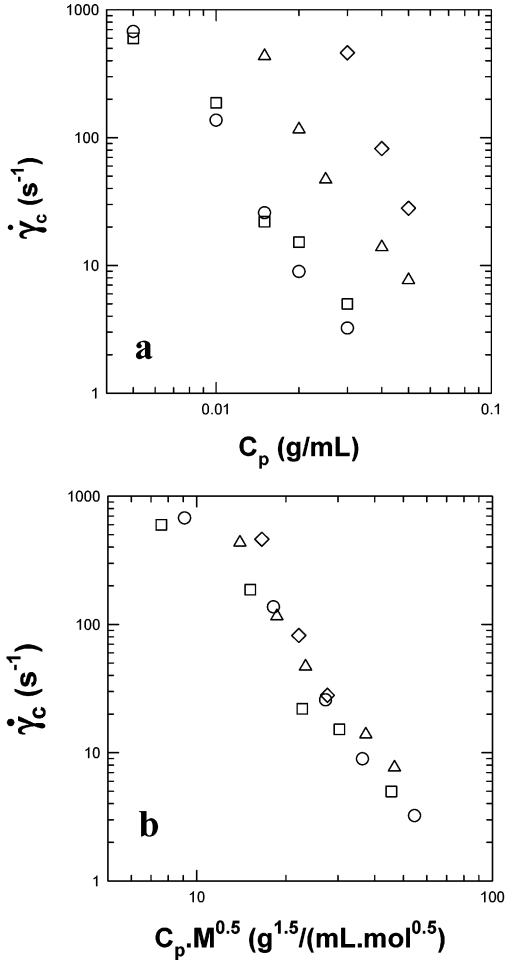

Figure 8. Concentration dependence of the critical shear rate for various molecular weights of 80DMA/10AA/10C12 (a) and after a rescaling of the concentration with $M^{0.5}$ (b). Symbols are the same as in Figure 3.

The shear thickening is measured for concentrations close to the crossover concentration regime defined previously (limit between domains I and II). When the concentration increases, the shear thickening appears at lower $\dot{\gamma}_c$ and the amplitude of the effect is obviously less pronounced since solutions already behave as physical gels at rest.

We have succeeded in measuring shear thickening only for polymers having a molecular weight higher than 300 kg/mol. Figure 8a shows the concentration dependence of $\dot{\gamma}_c$ for various molecular weights of 80DMA/10AA/10C12. Whatever the molecular weight is, $\dot{\gamma}_c$ decreases sharply with concentration ($\dot{\gamma}_c \approx C_p^{-3}$). Nevertheless, for a given concentration the shear thick-

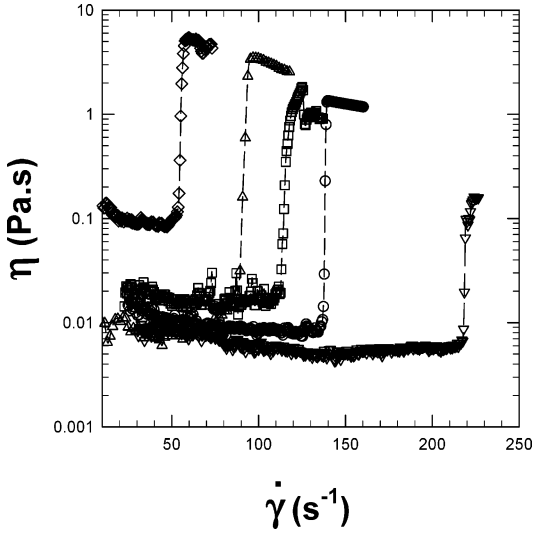

Figure 9. Rheograms obtained for 80DMA/(20 − *y*)AA/*y*C12 at 0.01 g/mL with $y = 1$ (◇), 2 (△), 5 (□), 10 (○), and 15 mol % (▽).

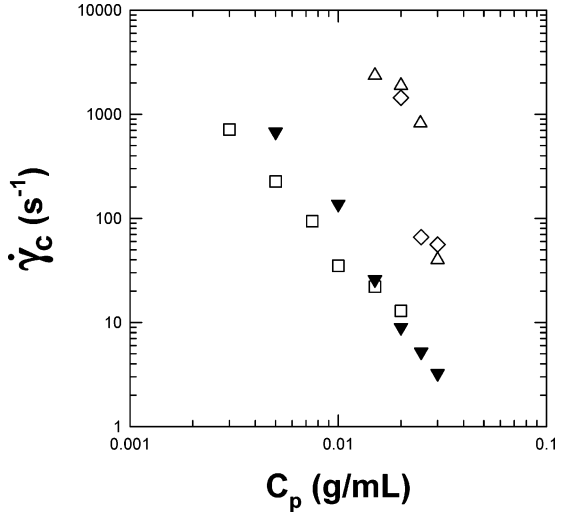

Figure 10. Concentration dependence of the critical shear rate for terpolymers with various charge densities. Symbols are the same as in Figure 6.

ening is easier to get as the molecular weight of the chains becomes higher. Actually it is possible to superimpose all the data on a single master curve by rescaling the concentration axis with the square root of M (Figure 8b).

Influence of the Composition of the Terpolymers.

Figure 9 shows rheograms obtained for 80DMA/(20 − *y*)AA/*y*C12 at a fixed concentration. The increase of $\dot{\gamma}_c$ with increasing grafting content is weak as it can be seen from the scale used for the shear rate axis. However, whatever the concentration, the more hydrophobic terpolymers show higher values for $\dot{\gamma}_c$. As discussed previously, at low concentration an increase of the hydrophobic content from 0 up to 15 mol % compacts the macromolecules. Thus, for a given concentration, the polymer volume fraction decreases when the hydrophobic content increases, which delays the appearance of shear thickening. The same conclusion can be drawn when for a fixed grafting content the size of the alkyl side chains increases. Furthermore, in the latter case the energy which is needed for an alkyl chain to escape from a hydrophobic microdomain is known to grow exponentially with the number of methylene groups involved.[17] Nevertheless, the shear-induced gelation of the hydrophobic terpolymers is more a gradual phenomenon than a critical one, which could be explained by the slowing down of the overall dynamics of the system when longer alkyl side chains are considered.

Figure 10 represents the concentration dependence of $\dot{\gamma}_c$ for terpolymers showing various charge densities. For a given concentration the increase of the number of charges borne by the polymer increases the critical shear rate. Furthermore, for the two highly charged terpolymers, the minimal concentration needed to observe shear thickening is higher since the crossover concentration between domains I and II increases with charge density.

V. Relaxation of the Shear-Induced Gels.

It is possible to characterize the mechanical properties of the gels once they are formed by measuring the time relaxation of the elastic modulus G' in the linear viscoelastic regime (1 Hz and 10% strain). The experimental results can be fitted with stretched exponentials according to $G'(t) = G_i \exp[-(t/\tau_g)^{\alpha}]$, with α being between 0.6 and 0.7. The small dispersion of the latter value allows comparison between the different systems. Both τ_g and the extrapolation to zero of $G'(t)$ ($G'(0)$) do not depend on the frequency, whereas $G''(0)$ decreases when the frequency increases. Such a result is expected when one considers a Maxwellian fluid at a frequency higher than the inverse of the relaxation time; G' is thus proportional to the number of elastically active chains. It can be concluded that $G'(0)$ corresponds to the plateau modulus of the gel induced under shear (G_0^g). It should be emphasized that τ_g corresponds to the characteristic time needed to lose the viscoelastic properties and does not necessarily correspond to a return back to the initial state of the solution.[8]

Figure 11 shows the concentration dependence of both G_0^g and τ_g for 80DMA/10AA/10C12 with various molecular weights. Measurements have been done at 10 °C to slow the relaxations and thus broaden both the molecular weight and the concentration ranges investigated. G_0^g does not depend systematically on the molecular weight, whereas τ_g definitively does. It can be seen that the network keeps the same topology whatever the molecular weight is, but its relaxation follows the variation $\tau_g \approx M^3$.

Influence of the Composition of the Terpolymers.

Let us first consider the series 80DMA/(20 − *y*)AA/*y*C12 (3100) at a fixed concentration (0.01 g/L). The plateau modulus of the induced gels does not depend on the alkyl content, and an average value of 40 Pa has been measured (results not shown). In the same way, the relaxation time is not affected by the alkyl content except for the lowest hydrophobically modified polymers which show values 1 order of magnitude lower. Thus, it can be deduced that the structure of the shear-induced gels remains the same for alkyl content higher than 2 mol %. This shows that above this value intramolecular associations (which delay the shear-induced gelation) are the only ones to get stronger and the "extra" added hydrophobic pendants do not take part to the overall elasticity of the network. The faster relaxation encountered with the lowest hydrophobic contents is not due to the smallest density of reticulation but is more the consequence of a weaker stability for the network, thanks to the small number of hydrophobic pendants that can take part in the looser intermolecular associations.

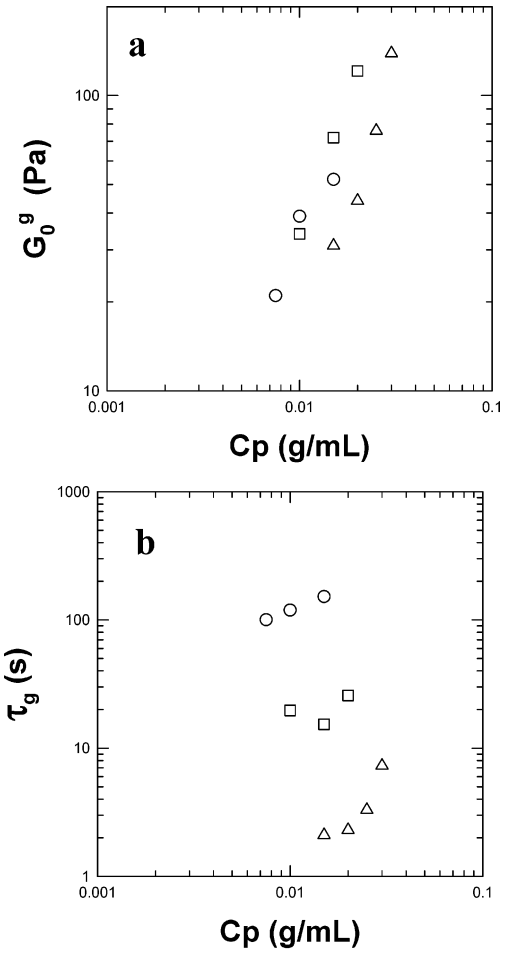

Figure 11. Concentration dependence of the plateau modulus G_0^g (a) and relaxation time τ_g (b) for the gels induced under shear with 80DMA/10AA/10C12 showing various molecular weights. Symbols are the same as in Figure 3. Measurements have been done at 10 °C (see text).

Keeping all the structural parameters constant except the size of the alkyl pendants, the same conclusions may be drawn: the plateau modulus of the induced gels does not change with the alkyl length. Again, 2 mol % of dodecyl side chains seems to be an optimal value; thus, adding more alkyl pendants has no consequence on the topological properties of the shear-induced gels. Nevertheless, the relaxation time is deeply affected by the alkyl length since it grows exponentially with the alkyl length (Figure 12). This behavior has already been measured on model associative thickeners by Annable et al.,[17] who showed that the relaxation time of a macroscopic strain is indicative for the lifetime of the alkyl pendants inside the hydrophobic microdomains. Nevertheless, in our case the relaxation times are almost 3 orders of magnitude higher than the ones measured by Annable et al. due to different molecular weight. Actually, even if the relaxation of the shear-induced gels implies a slower reorganization of the network, the latter is definitively driven by the lifetime of the alkyl side chains.

Discussion

As shown by the linear rheology measurements, two concentration regimes can be discriminated. At low concentrations the behavior of the hydrophobically modified polyelectrolytes is one of a nonentangled polyelectrolyte collapsed by intramolecular hydrophobic

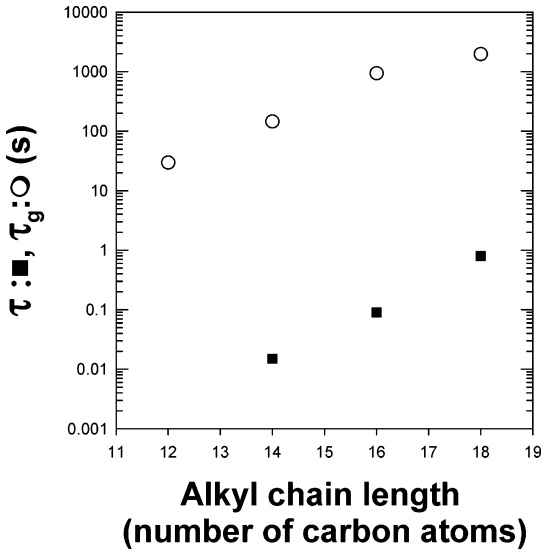

Figure 12. Influence of the length of the alkyl pendants on the relaxation time measured for the shear-induced gels based on the 80DMA/15AA/5C*n* (3100) series (○). Results are compared with the relaxation time measured by Annable et al.[17] on model associative thickeners (■, C_p = 4%; M_w = 35 000 g/mol).

associations. For higher concentrations (domain II) the polymers become entangled, which is concomitant with the transformation of intramolecular associations into intermolecular ones.

However, the charge density—at constant hydrophobicity—leads to a decrease of the viscosity and an increase of the crossover concentration I—II, which are striking results.

This behavior can be understood if one now assumes that in regime I chains are not isolated but involved in small aggregates. In a further publication we will report clear evidence for this fact. Let us now discuss the effect of hydrophobicity and charge density on the chain aggregation number.

The hydrophobicity has the tendency to increase this aggregation number, but the charge density has an opposite effect. This situation is somehow reminiscent to the behavior encountered with charged wormlike micelles. In that case, the tendency for surfactant to make long wormlike micelles is counterbalanced by the electrostatic repulsion.[36]

Thus, it is reasonable to think that increasing the charge density decreases the size of the chain aggregates. This simple remark allows explaining the viscosity dependence on the charge density.

In addition, the effect of concentration on charged wormlike micelles is not straightforward. Two regimes clearly appear. At low concentration the objects consist in nonentangled small cylinders whose growth with concentration is very weak. At higher concentration the objects consist in very long entangled cylinders and their growth exhibits a strong—exponential—increase of the length with concentration. This phenomenon is due to the change in the electrostatic screening at the overlap concentration. At low concentration the objects are individual small cylindrical micelles and the range of the electrostatic interactions is roughly the distance between neighboring objects and thus larger than the length of the cylinders. At high concentration the micelles become entangled and the electrostatic interactions range is the distance between nearest cylinder:

the radius of the "tube" constituted by the neighboring micelles. Thus, this electrostatic range is smaller than the size of the micelles and screened by its neighbors; the growth law becomes then very different. The transition between the two regimes is sharper and sharper if one increases the charge density while the crossover concentration increases.

We believe that this picture can be transposed to our system. The charge density competes with the hydrophobic interactions to control the size of the chain aggregates. In the dilute regime, the size of the aggregates depends weakly on concentrations, but at higher concentration, when the aggregates begin to overlap, an electrostatic screening may develop, leading to a dramatic increase of the size of the aggregates. This does not mean for us that the aggregates encountered with our terpolymers are wormlike, but we would rather like to point out the important change of electrostatic interactions around the overlap concentration. This leads to a sharp increase of the viscosity—see Figure 6—that cannot be accounted for by the single transformation of an intra- into interassociation model.

This suggests that the crossover regime between domains I and II, in the case of highly charged polymer (>10 mol %), can be viewed as follows. In domain I small elongated aggregates involving several chains grow slowly with concentration as the electrostatic interactions are larger than their sizes. Then at a given concentration, for energetical purposes, aggregates may overlap, which leads to the formation of a network based on chains connected via hydrophobic microdomains. At the same time the electrostatic range becomes the mesh size of this network

Similar to the case of wormlike micelles, we believe that that this "transition" may be induced by a shear flow. Actually in wormlike micelles it has been observed that when the systems are charged they exhibit a shear-induced gelation qualitatively similar to ours. It has been claimed that shear thickening was due to the shear-induced formation of structures with large dimension, thanks to the end-to-end fusion of orientated rodlike micelles. Nevertheless, a recent and detailed study carried on fluorocarbon surfactants[37] suggests a ring-driven mechanism.[38]

Finally, despite numerous experimental and theoretical studies, this phenomenon remains unclear, but experimental evidence clearly relates the sharp growth of the micelles at the crossover concentration to the existence of a shear-induced gelation. Thus, it is likely that shear induces the transition between the isolated small cylinders and the entangled self-screened worms. We suggest that the same picture also holds for our systems. Different experimental facts may support this idea. First, the effect of shear is sharper when the charge content increases. In the same way, in the linear regime, the transition from domain I to domain II is sharper when the charge content increases. Second, the shear-induced gelation vanishes when the second concentration domain is reached (see Figure 7 at the highest concentration). Last, the shear-induced gels display the same properties in terms of relaxation time and modulus as the phase in domain II. Hence, we suggest that hydrophobically modified charged terpolymers exhibit a shear-induced gelation reminiscent of charged wormlike micelles.

Conclusion

We synthesized a series of hydrophobically modified amphiphilic polymers which exhibit reversible shear-induced gelation properties. At rest and low concentration, the hydrophobic modification compacts the macromolecules thanks to intramolecular associations. As the concentration increases further on, the sharp increase of both the viscosity and the terminal relaxation time can be understood in terms of the turn-up of intramolecular associations into intermolecular ones as evidenced from the fair agreement between experimental results and theoretical predictions for such a transition for a series of weakly charged polymers. The molecular features that increase the compaction of the macromolecules at rest, i.e., an increase of hydrophobic content, delay this transition in terms of concentration. Under shear, pronounced shear-induced gelations have been measured and quantitatively described through the value for the critical shear rate ($\dot{\gamma}_c$). From a structural point of view, an increase of the hydrophobic and/or of the charge content delays the shear-induced gelation.

A parallel may be drawn between our systems and wormlike micelles. From the static point of view the size of the aggregates is the result of an equilibrium between attractive hydrophobic interactions and repulsive electrostatic ones. The electrostatic screening, which increases with concentration, leads to a sharp increase of the size of the aggregates and as a consequence in a sharper crossover regime between domains I and II. From the dynamic point of view such a transition is favored under shear. We are fully aware that molecular insights regarding this shear-induced gelation are still missing, but we will report soon results that will confront the macroscopic parameters measured here with information gained at the mesoscopic level thanks to light-scattering measurements.

Acknowledgment. The authors acknowledge the funding of this project by Schlumberger Dowell. Furthermore, they thank G. Bokias, G. Ducouret, I. Iliopoulos, and D. Hourdet for helpful discussions. Last, they are grateful to Drs. M. Badiger and P. P. Wadgaonkar for their careful reading of the manuscript.

References and Notes

(1) Barnes, H. A.; Hutton, J. F.; Walters, K. *An introduction to rheology*; Elsevier: New York, 1989.
(2) Liu, S. F.; Lafuma, F.; Audebert, R. *Colloid Polym. Sci.* **1993**, *272*, 196−203.
(3) Escalante, J.; Hoffmann, H. *J. Phys.: Condens. Matter* **2000**, *12*, 483−489.
(4) Léon, A.; Bonn, D.; Meunier, J.; Al-Kahwaji, A.; Greffier, O.; Kellay, H. *Phys. Rev. Lett.* **2000**, *84*, 1335−1338.
(5) Panizza, P.; Colin, A.; Coulon, C.; Roux, D. *Eur. Phys. J. B* **1998**, *4*, 65−74.
(6) Hu, Y.; Wang, S. Q.; Jamieson, A. M. *J. Rheol.* **1993**, *37*, 531−546.
(7) Berret, J. F.; Gamez-Corrales, R.; Oberdisse, J.; Walker, L. M.; Lindner, P. *Europhys. Lett.* **1998**, *41*, 677−682.
(8) Oda, R.; Weber, V.; Lindner, P.; Pine, D. J.; Mendes, E.; Schosseler, F. *Langmuir* **2000**, *16*, 4859−4863.
(9) Layec-Raphalen, M. N.; Wolff, C. *J. Non-Newtonian Fluid Mech.* **1976**, *1*, 159−173.
(10) Yanase, H.; Moldanaers, P.; Mewis, J.; VanEgmond, J.; Fuller, G. *Rheol. Acta* **1991**, *30*, 89−97.
(11) Moldenaers, P.; Yanase, H.; Mewis, J.; Fuller, G.; Lee, C.-S.; Magda, J. J. *Rheol. Acta* **1993**, *32*, 1−8.
(12) Vrahopoulou, E. P.; McHugh, A. J. *J. Non-Newtonian Fluid Mech.* **1987**, *25*, 157−175.

(13) Dupuis, D.; Lewandowski, F. Y.; Steiert, P.; Wolff, C. *J. Non-Newtonian Fluid Mech.* **1994**, *54*, 11−32.
(14) Eliassaf, J.; Silberberg, A.; Katchalsky, A. *Nature* **1955**, *176*, 1119−1119.
(15) Onuki, A. *J. Phys.: Condens. Matter* **1997**, *9*, 6119−6157.
(16) Winnik, M. A.; Yekta, A. *Curr. Opin. Colloid Interface Sci.* **1997**, *2*, 424−436.
(17) Annable, T.; Buscall, R.; Ettelaie, R.; Whittlestone, D. *J. Rheol.* **1993**, *37*, 695−726.
(18) Tam, K. C.; Jenkins, R. D.; Winnik, M. A.; Bassett, D. R. *Macromolecules* **1998**, *31*, 4149−4159.
(19) Lundberg, D. J.; Glass, J. E.; Eley, R. R. *J. Rheol.* **1991**, *35*, 1255−1274.
(20) Ma, S. X.; Cooper, S. L. *Macromolecules* **2001**, *34*, 3294−3301.
(21) Marrucci, G.; Bhargava, S.; Cooper, S. L. *Macromolecules* **1993**, *26*, 6, 6483−6488.
(22) Witten, T. A.; Cohen, M. H. *Macromolecules* **1985**, *18*, 1915−1918.
(23) Witten, T. A. *J. Phys. Fr.* **1988**, *49*, 1055−1063.
(24) Bokias, G.; Hourdet, D.; Iliopoulos, I. *Macromolecules* **2000**, *33*, 2929−2935.
(25) Goveas, J. L.; Pine, D. J. *Europhys. Lett.* **1999**, *48*, 706−712.
(26) Léon, A.; Bonn, D.; Meunier, J.; Al-Kahwaji, A.; Kellay, H. *Phys. Rev. Lett.* **2001**, *86*, 938−941.
(27) Bokias, G.; Durand, A.; Hourdet, D. *Macromol. Chem. Phys.* **1998**, *199*, 1387−1392.
(28) Bulai, A.; Jimeno, M. L.; Alencar de Queiroz, A. A.; Gallardo, A.; San Roman, J. *Macromolecules* **1996**, *29*, 3240−3246.
(29) Bulai, A.; Alencar de Queiroz, A. A.; Gallardo, A.; San Roman, J. *Polymer* **1999**, *40*, 4953−4960.
(30) Miron, Y.; Morawetz, H. *Macromolecules* **1969**, *2*, 162−165.
(31) Cabaness, W. R.; Yen-Chin Lin, T.; Parkanyi, C. *J. Polym. Sci.* **1971**, *9*, 2155−2170.
(32) Jimenez Regalado, E.; Selb, J.; Candau, F. *Macromolecules* **1999**, *32*, 8580−8588.
(33) Rubinstein, M.; Semenov, A. *Macromolecules* **2001**, *34*, 1058−1068.
(34) Dobrynin, A. V.; Colby, R. H.; Rubinstein, M. *Macromolecules* **1995**, *28*, 1859−1871.
(35) English, R. J.; Gulati, H. S.; Jenkins, R. D.; Khan, S. A. *J. Rheol.* **1997**, *41*, 427−444.
(36) MacKintosh, F. C.; Safran, S. A.; Pincus, P. A. *Europhys. Lett.* **1990**, *12*, 697−702.
(37) Oelschlaeger, C.; Waton, G.; Buhler, E.; Candau, S. J.; Cates, M. E. *Langmuir* **2002**, *18*, 3076−3085.
(38) Cates, M. E.; Candau, S. J. *Europhys. Lett.* **2001**, *55*, 887−893.

MA0482258